

Analysis of Kerr frequency combs in microresonators with two-photon absorption and free-carriers

Lukas Bengel and Wolfgang Reichel

Abstract We study optical Kerr frequency combs in nonlinear microresonators in the presence of two-photon absorption (TPA) and free-carrier absorption (FCA) described by an extended Lugiato-Lefever system of equations. We give a criterion for modulation instability of constant stationary solutions and establish existence of non-constant solutions. Both results are accompanied by numerical simulations, which show that the abstract conditions both for modulation instability and existence are satisfied in large parts of the parameter regions.

1 Introduction

Kerr frequency combs in nonlinear microresonators are versatile tools for a wide field of applications ranging from optical communications [16], spectroscopy [22], ultrafast optical measurements [22, 23] to high precision clocks [4, 25]. The typical design of a Kerr nonlinear microresonator is based on specifically composed silica and silicon nitride waveguides. Frequency combs, i.e., stable signals which are highly localized in time-domain and have a broad and equally spaced spectral signature in frequency domain, emerge under suitable operating conditions of the microresonator as the outcome of nonlinear interaction of the resonantly enhanced pump field leading to modulation instability, and, ultimately to the formation of a stable stationary pattern. The mathematical model [1, 2, 13] for the dynamics of frequency combs is known as the Lugiato-Lefever equation,

Lukas Bengel
Institute for Analysis (IANA), Karlsruhe Institute of Technology, 76131 Karlsruhe, Germany,
e-mail: lukas.bengel@kit.edu

Wolfgang Reichel
Institute for Analysis (IANA), Karlsruhe Institute of Technology, 76131 Karlsruhe, Germany,
e-mail: wolfgang.reichel@kit.edu

$$ia_t(x, t) = -da_{xx}(x, t) + (\zeta - i - |a(x, t)|^2)a(x, t) + if \quad (1)$$

which is a damped, driven and detuned nonlinear Schrödinger equations. Here $a = a(x, t)$ with $(x, t) \in [0, L] \times \mathbb{R}$ represents the optical field inside a ringresonator of length L which is coupled to a continuous strong input laser and subject to damping losses and material dispersion. The material dispersion is given by d ($d < 0$ stands for normal dispersion, $d > 0$ for anomalous dispersion), the forcing by f (arising from the continuous strong laser source), and the damping term by $-ia$ (describing losses). Additionally, there is a detuning variable ζ , which describes the offset between the frequency of the input laser and the nearest resonance frequency of the linear dispersion relation of the ringresonator.

There has been a lot of results in the physics, engineering, and mathematical literature about the properties of (1). Although not at the center of our interest in this paper, let us briefly indicate some results which are in the same spirit as the ones we shall present. The most elementary states of (1) are those, where only the pumped mode is excited and no other mode of the ringresonator. These states are given as spatially constant steady states of (1). Of interest are of course spatially localized states, and they can be investigated, e.g., via bifurcation analysis from spatially constant states as in [7, 15, 17, 18, 19, 20] or via their dynamical stability/instability properties as in [3, 8, 10, 12, 21].

Recently, new designs of Kerr microresonators based on silicon have entered scientific discussions. Their advantage is the well-established material platform and the much higher Kerr effect. However, there are drawbacks: two-photon absorption (TPA) and free-carrier absorption (FCA). TPA describes the effect that two photons simultaneously excite an electron from the valence band into the conduction band. Within the conduction band additional photons can excite the electrons into even higher excitation states (FCA). Altogether, TPA and FCA act against Kerr comb formation due to their cumulative damping effect. This effect leads to a coupled model, where next to the optical field $a = a(x, t)$ also the free-carrier density $N = N(x, t)$ needs to be considered. In (1) the reference frame has already been chosen such that stationarity on (1) amounts to movement with group-velocity v . Since free carriers do not move with the optical field, the reference frame of the free carrier density $N = N(x, t)$ is retarded relative to a . As a result, cf. [11, 14, 24], the following model has been derived

$$\begin{aligned} ia_t(x, t) &= -da_{xx}(x, t) + (\zeta - i - (1 + ir)|a(x, t)|^2)a(x, t) + if, \\ &\quad - \sigma(i - \mu)N(x - tv, t)a(x, t), \\ N_t(x, t) &= r|a(x + tv, t)|^4 - \frac{N(x, t)}{\tau}. \end{aligned} \quad (2)$$

Here, $\tau > 0$ is the effective life-time (dwell time) of the free carriers, $r > 0$ quantifies the TPA effect, $\sigma > 0$ is the FCA cross section, and $\mu \in \mathbb{R}$ the FCA dispersion. Notice the relative retardation of N in the first equation and the relative advancement of a in the second equation.

A mathematically simple way to remove the relative retardation is to define $n(x, t) = N(x - tv, t)$ as the moving coordinate version of the free carrier density. The resulting equation is then given by

$$\begin{aligned} ia_t &= -da_{xx} + (\zeta - i - \sigma(i - \mu)n - (1 + ir)|a|^2)a + if, \\ n_t &= r|a|^4 - vn_x - \frac{n}{\tau}, \end{aligned} \quad (3)$$

and it is this equation on which we base our analysis. It is easy to see that homogeneous steady states $n_0 \in \mathbb{R}$ and $a_0 \in \mathbb{C}$ of (3) exists and satisfy

$$(\zeta - i - \sigma(i - \mu)n_0 - (1 + ir)|a_0|^2)a_0 + if = 0, \quad r|a_0|^4 - \frac{n_0}{\tau} = 0. \quad (4)$$

It is reasonable to conjecture that the additional effects caused by TPA and FCA may prevent the existence of other, non-constant steady states – provided $r, \sigma > 0$ are too large. The only way to counterbalance this is the value of the dwell time τ . Indeed, on a technical level, the free carriers can be removed from the microresonator by a reverse biased p-i-n-junction so that their dwell time within the device can be substantially reduced.

The goal of this paper is two-fold.

- (i) We will provide conditions on the parameters $\zeta, \sigma, \tau, d, \mu$ such that a steady state (a_0, n_0) of (3) becomes unstable. This instability can be seen as the onset of the formation of non-trivial, patterned states which ultimately lead to frequency combs. This is done in Theorem 1 in Section 2, and it provides a rigorous backup to a very similar result obtained in [24] based on a substantial number of physically well-justified but mathematically non-rigorous approximations.
- (ii) We will give rigorous existence results for particular non-homogeneous solutions of (3). This is done in Theorem 3 in Section 3. We are not aware of any other existence results for (3) except for [5], where a much simplified version with TPA but without FCA has been studied. Our result build upon [5] and show existence for values of σ and μ near zero by a bifurcation argument based on the Lyapunov-Schmidt reduction.

Our results are illustrated with numerical simulations. We finish the paper with a discussion and conclusion in Section 4.

2 Modulation instability of constant steady states

Constant steady states of (3) are solutions $(a_0, n_0) \in \mathbb{C} \times \mathbb{R}$ of the algebraic equations (4). Note that $|a_0|^2$ is related to the forcing f by

$$\left((\zeta + \sigma\mu r\tau|a_0|^4 - |a_0|^2)^2 + (1 + \sigma r\tau|a_0|^4 + r|a_0|^2)^2 \right) |a_0|^2 = f^2. \quad (5)$$

Linearization of (3) about a constant steady state $(a_0, n_0) \in \mathbb{C} \times \mathbb{R}$ yields

$$\begin{aligned} ia_t &= -da_{xx} + (\zeta - i - \sigma(i - \mu)n_0)a - \sigma(i - \mu)a_0n - (1 + ir)(2|a_0|^2a + a_0^2\bar{a}), \\ n_t &= 2r|a_0|^2(a_0\bar{a} + \bar{a}_0a) - vn_x - \frac{n}{\tau}. \end{aligned}$$

In the following we will look for conditions which yield exponentially growing solutions of the linearized equations. This phenomenon is called modulation instability. Our investigation of modulation instability consists of analytical results in Section 2.1 and numerical illustrations in Section 2.2.

2.1 Analysis of the linearized equations

In the equation for a there is a coupling between a and its complex conjugate \bar{a} . For n the situation is different since $n = \bar{n}$, provided $n(\cdot, 0)$ is a real-valued and hence physical initial condition. Nevertheless, it is helpful to adjoin the following equations both for \bar{a} and \bar{n} to the previous two equations

$$\begin{aligned} -i\bar{a}_t &= -d\bar{a}_{xx} + (\zeta + i + \sigma(i + \mu)n_0)\bar{a} + \sigma(i + \mu)\bar{a}_0\bar{n} - (1 - ir)(2|a_0|^2\bar{a} + \bar{a}_0^2a), \\ \bar{n}_t &= 2r|a_0|^2(\bar{a}_0a + a_0\bar{a}) - v\bar{n}_x - \frac{\bar{n}}{\tau} \end{aligned}$$

so that altogether we obtain a system of four equations for (a, \bar{a}, n, \bar{n}) . Using the notation $\mathbb{T} = \mathbb{R}/2\pi\mathbb{Z}$ for the one dimensional torus of length 2π we define next the following differential operators

$$\begin{aligned} A : H^2(\mathbb{T}) &\rightarrow L^2(\mathbb{T}) \text{ with } A := -d\partial_x^2 + \zeta - i - \sigma(i - \mu)n_0 - (1 + ir)2|a_0|^2, \\ B : (H^2(\mathbb{T}))^2 \times (H^1(\mathbb{T}))^2 &\rightarrow (L^2(\mathbb{T}))^4 \text{ with} \\ B &:= \begin{bmatrix} A & -(1 + ir)a_0^2 & -\sigma(i - \mu)a_0 & 0 \\ -(1 - ir)\bar{a}_0^2 & A^* & 0 & \sigma(i + \mu)\bar{a}_0 \\ 2r|a_0|^2\bar{a}_0 & 2r|a_0|^2a_0 & -v\partial_x - \frac{1}{\tau} & 0 \\ 2r|a_0|^2\bar{a}_0 & 2r|a_0|^2a_0 & 0 & -v\partial_x - \frac{1}{\tau} \end{bmatrix}. \end{aligned}$$

Then the operator

$$L := JB : (H^2(\mathbb{T}))^2 \times (H^1(\mathbb{T}))^2 \rightarrow (L^2(\mathbb{T}))^4 \text{ with } J := \text{diag}(-i, i, 1, 1) \in \mathbb{C}^{4 \times 4} \quad (6)$$

allows us to write the linearized equation as

$$\mathbf{v}_t = L\mathbf{v}, \quad \mathbf{v} = (a, \bar{a}, n, \bar{n})^\top.$$

We will show that under certain conditions on the parameters, specified in the theorem below, there exist (spectrally) unstable constant steady states, i.e., $\sigma(L) \cap \{z \in \mathbb{C} : \text{Re } z > 0\} \neq \emptyset$. For the statement of the following theorem we use the notation $[x]$ to denote the closest integer to $x \in \mathbb{R}$ (if x has distance $1/2$ from the integers one may pick either of the neighbouring integers).

Theorem 1 Let $d \in \mathbb{R} \setminus \{0\}$, $r, \sigma, \tau > 0$, $\mu, v, \zeta, f \in \mathbb{R}$, and $\epsilon > 0$ be given parameters and assume that $(a_0, r\tau|a_0|^4) \in \mathbb{C} \times \mathbb{R}$ is a steady state of (3). Define

$$k^* := \left\lceil \sqrt{\frac{2|a_0|^2 - \sigma\mu r\tau|a_0|^4 - \zeta}{d}} \right\rceil, \quad \Delta := \frac{d(k^*)^2 + \zeta}{|a_0|^2} + \sigma\mu r\tau|a_0|^2 - 2.$$

Then the steady state $(a_0, r\tau|a_0|^4) \in \mathbb{C} \times \mathbb{R}$ is spectrally unstable provided the following three conditions hold:

$$2r < \sqrt{1+r^2-\Delta^2}, \quad \sigma\tau < \frac{1}{(1+\epsilon)4r} \left(\sqrt{1+r^2-\Delta^2} - 2r \right)^2 \quad (7)$$

and

$$|a_0|^2 \in (\xi_1(\epsilon), \xi_2(\epsilon)) \quad (8)$$

where $0 < \xi_1(\epsilon) < \xi_2(\epsilon)$ denote the roots of the polynomial

$$q_\epsilon(\xi) = -1 - \epsilon + (\sqrt{1+r^2-\Delta^2} - 2r)\xi - \sigma r\tau\xi^2$$

and

$$\left(\epsilon + \frac{|\omega_1| + |\omega_4|}{\epsilon} \right)^2 < \left(-1 + (\sqrt{1+r^2-\Delta^2} - 2r)|a_0|^2 - \sigma r\tau|a_0|^4 + \frac{1}{\tau} \right)^2 + \frac{v^2|a_0|^2}{|d|} \quad (9)$$

where

$$\omega_1 := \frac{2\sigma r|a_0|^4}{(1+r^2-\Delta^2)} \left((r - \mu(1+\Delta))\sqrt{1+r^2-\Delta^2} - (1+r^2-\Delta^2) \right),$$

$$\omega_4 := \frac{2\sigma r|a_0|^4}{(1+r^2-\Delta^2)} \left((\mu(1+\Delta) - r)\sqrt{1+r^2-\Delta^2} - (1+r^2-\Delta^2) \right).$$

Moreover, the instability appears for modes with wave number k^* .

Remark 1 We have implicitly assumed that the expressions in the two square roots of the above theorem are non-negative.

Proof. Using the notation from (6), let L denote the linearization about the steady state $(a_0, r\tau|a_0|^4)$. Exploiting the Fourier transform of periodic L^2 -functions we decompose the spectrum of the linearization

$$\sigma(L) = \bigcup_{k \in \mathbb{Z}} \sigma(L_k)$$

where the matrices L_k are given by

$$L_k = \begin{bmatrix} \ell_1(k) & \ell_2 & \ell_3 & 0 \\ \bar{\ell}_2 & \bar{\ell}_1(k) & 0 & \bar{\ell}_3 \\ \bar{\ell}_4 & \ell_4 & \ell_5(k) & 0 \\ \bar{\ell}_4 & \ell_4 & 0 & \ell_5(k) \end{bmatrix} \in \mathbb{C}^{4 \times 4},$$

with coefficients

$$\begin{aligned} \ell_1(k) &= -idk^2 - (i\zeta + 1) - \sigma r \tau (1 + i\mu) |a_0|^4 + 2(i-r) |a_0|^2, & \ell_2 &= (i-r) a_0^2, \\ \ell_3 &= -\sigma(1 + i\mu) a_0, & \ell_4 &= 2r |a_0|^2 a_0, & \ell_5(k) &= -ivk - \frac{1}{\tau}. \end{aligned}$$

In particular, it is enough to show that there exists $k \in \mathbb{Z}$ such that $\sigma(L_k) \cap \{z : \operatorname{Re} z > 0\} \neq \emptyset$. Let us fix some $k \in \mathbb{Z}$ and consider the matrix L_k . To get a better understanding of the spectrum of L_k we perform several similarity transformations, eventually allowing us to locate eigenvalues of the matrix. If we define $T_1 = \operatorname{diag}(1, 1, \ell_3, \bar{\ell}_3) \in \mathbb{C}^{4 \times 4}$ then one finds

$$L_{1,k} := T_1 L_k T_1^{-1} = \begin{bmatrix} \ell_1(k) & \ell_2 & 1 & 0 \\ \bar{\ell}_2 & \bar{\ell}_1(k) & 0 & 1 \\ \ell_3 \bar{\ell}_4 & \ell_3 \ell_4 & \ell_5(k) & 0 \\ \bar{\ell}_3 \bar{\ell}_4 & \bar{\ell}_3 \ell_4 & 0 & \ell_5(k) \end{bmatrix}.$$

The matrix

$$A_k := \begin{bmatrix} \ell_1(k) & \ell_2 \\ \bar{\ell}_2 & \bar{\ell}_1(k) \end{bmatrix}$$

has the eigenvalues

$$\begin{aligned} \lambda_{\pm}(k) &= \operatorname{Re} \ell_1(k) \pm \sqrt{(\operatorname{Re} \ell_1(k))^2 - |\ell_1(k)|^2 + |\ell_2|^2} \\ &= -1 - \sigma r \tau |a_0|^4 - 2r |a_0|^2 \\ &\quad \pm \sqrt{|a_0|^4 (1 + r^2) - (dk^2 + \zeta + \sigma \mu r \tau |a_0|^4 - 2|a_0|^2)^2}. \end{aligned}$$

Observe that

$$\max\{\operatorname{Re} \lambda_{\pm}(k) : k \in \mathbb{Z}\} = \lambda_+(\pm k^*) = -1 + |a_0|^2 \left(\sqrt{1 + r^2 - \Delta^2} - 2r \right) - \sigma r \tau |a_0|^4,$$

where $k^* = \left\lceil \frac{\sqrt{(2|a_0|^2 - \sigma \mu r \tau |a_0|^4 - \zeta)/d}}{d} \right\rceil$ is the integer which is closest to $\frac{\sqrt{(2|a_0|^2 - \sigma \mu r \tau |a_0|^4 - \zeta)/d}}{d}$. Thus anticipating that L_{k^*} has an unstable eigenvalue close to $\lambda_+(\pm k^*)$ we will from now on set $k = k^*$.

The matrix A_{k^*} is diagonalizable through conjugation with the matrix

$$S := \begin{bmatrix} a_0^2(i-r) & a_0^2(i-r) \\ |a_0|^2(\sqrt{1+r^2-\Delta^2}+i\Delta) & |a_0|^2(-\sqrt{1+r^2-\Delta^2}+i\Delta) \end{bmatrix}.$$

Consequently, after introducing the block diagonal matrix $T_2 = \text{diag}(S, S) \in \mathbb{C}^{4 \times 4}$ we obtain

$$L_{2,k^*} = T_2^{-1} L_{1,k^*} T_2 = \begin{bmatrix} \lambda_+(k^*) & 0 & 1 & 0 \\ 0 & \lambda_-(k^*) & 0 & 1 \\ \omega_1 & \omega_2 & \ell_5(k^*) & 0 \\ \omega_3 & \omega_4 & 0 & \ell_5(k^*) \end{bmatrix}$$

where the coefficients ω_i are computed from

$$\begin{bmatrix} \omega_1 & \omega_2 \\ \omega_3 & \omega_4 \end{bmatrix} = S^{-1} \begin{bmatrix} \ell_3 \bar{\ell}_4 & \ell_3 \ell_4 \\ \bar{\ell}_3 \bar{\ell}_4 & \bar{\ell}_3 \ell_4 \end{bmatrix} S.$$

The eigenvalues of L_{2,k^*} are precisely the roots of the characteristic polynomial

$$\begin{aligned} p(\lambda) &= \det(L_{2,k^*} - \lambda) \\ &= (\lambda_+(k^*) - \lambda)(\lambda_-(k^*) - \lambda)(\ell_5(k^*) - \lambda)^2 - \omega_1(\lambda_-(k^*) - \lambda)(\ell_5(k^*) - \lambda) \\ &\quad - \omega_4(\lambda_+(k^*) - \lambda)(\ell_5(k^*) - \lambda). \end{aligned}$$

Clearly, $p(\ell_5(k^*)) = 0$ which implies that $\ell_5(k^*)$ is a stable eigenvalue of L_{2,k^*} . The remaining roots of p are determined from the equation $\tilde{p}(\lambda) = 0$ where

$$\tilde{p}(\lambda) = (\lambda_+(k^*) - \lambda)(\lambda_-(k^*) - \lambda)(\ell_5(k^*) - \lambda) - \omega_1(\lambda_-(k^*) - \lambda) - \omega_4(\lambda_+(k^*) - \lambda).$$

To locate the roots of \tilde{p} , we observe that they coincide with the eigenvalues of the matrix

$$L_{3,k^*,\epsilon} := \begin{bmatrix} \lambda_+(k^*) & 0 & \epsilon \\ 0 & \lambda_-(k^*) & \epsilon \\ \frac{\omega_1}{\epsilon} & \frac{\omega_4}{\epsilon} & \ell_5(k^*) \end{bmatrix} \quad \text{for arbitrary } \epsilon > 0,$$

and where ω_1, ω_4 are the values given in the statement of the theorem.

The following result allows us to derive bounds on the location of the eigenvalues of $L_{3,k^*,\epsilon}$.

Theorem 2 (Gerschgorin's Circle Theorem, cf. [6])

Let $N \in \mathbb{N}$, $A = (a_{ij})_{i,j=1,\dots,N} \in \mathbb{C}^{N \times N}$ and $G_i := \{z \in \mathbb{C} : |z - a_{ii}| \leq \sum_{j:j \neq i} |a_{ij}|\}$. Then we have

$$\sigma(A) \subset \bigcup_{i=1}^N G_i.$$

Moreover, if $G_i \cap G_j = \emptyset$ for fixed i and all $j \neq i$, then $\sigma(A) \cap G_i \neq \emptyset$.

The Gerschgorin circles of $L_{3,k^*,\epsilon}$ are given by

$$\begin{aligned} G_1 &= \{z \in \mathbb{C} : |z - \lambda_+(k^*)| \leq \epsilon\}, \\ G_2 &= \{z \in \mathbb{C} : |z - \lambda_-(k^*)| \leq \epsilon\}, \\ G_3 &= \left\{ z \in \mathbb{C} : |z - \ell_5(k^*)| \leq \frac{|\omega_1| + |\omega_4|}{\epsilon} \right\}. \end{aligned}$$

We aim to show that

$$G_1 \subset \{z \in \mathbb{C} : \operatorname{Re} z > 0\}, \quad (10)$$

$$G_1 \cap G_2 = \emptyset, \quad (11)$$

$$G_1 \cap G_3 = \emptyset, \quad (12)$$

which, using Theorem 2, implies that $G_1 \cap \sigma(L_{3,k^*,\epsilon}) \neq \emptyset$, and the instability of $(a_0, r\tau|a_0|^4)$ then follows from $\sigma(L_{3,k^*,\epsilon}) \subset \sigma(L_{k^*}) \subset \sigma(L)$. To prove (10) let us consider the polynomial

$$q_\epsilon(\xi) = -1 - \epsilon + (\sqrt{1+r^2-\Delta^2} - 2r)\xi - \sigma r \tau \xi^2.$$

A short calculation shows that q_ϵ has two positive roots $0 < \xi_1(\epsilon) < \xi_2(\epsilon)$ if and only if

$$2r < \sqrt{1+r^2-\Delta^2}, \quad 0 < \sigma r < \frac{1}{(1+\epsilon)4r} \left(\sqrt{1+r^2-\Delta^2} - 2r \right)^2,$$

which is precisely (7). Consequently, we find $\lambda_+(k^*) > \epsilon$ provided $|a_0|^2 \in (\xi_1(\epsilon), \xi_2(\epsilon))$, which yields the inclusion (10). The explicit formula for $\lambda_-(k^*)$ also shows that $\lambda_-(k^*) \leq -\epsilon$, thus implying $|\lambda_+(k^*) - \lambda_-(k^*)| > 2\epsilon$ so that we have established (11). Finally, (12) follows from $\epsilon + \frac{|\omega_1|+|\omega_4|}{\epsilon} < |\lambda_+(k^*) - \ell_5(k^*)|$ which is equivalent to our assumption (9). Thus, the proof of Theorem 1 is complete. \square

Remark 2 Assumption (7) in Theorem 1 yields an upper bound for the TPA parameter since

$$2r < \sqrt{1+r^2-\Delta^2} \leq \sqrt{1+r^2} \implies r < \frac{1}{\sqrt{3}}.$$

In the context of instabilities of steady-states for (2) this bound was already derived in [5, 24].

In the case of anomalous dispersion $d > 0$, a simplified version of Theorem 1 can be obtained as follows. First, by optimizing the detuning parameter $\zeta \in \mathbb{R}$ in such a way that $\zeta = A - \sigma\mu r\tau A^2$, $A = |a_0|^2$ we obtain the maximal power transfer between the forcing f and the power A of the $k = 0$ -mode. The above choice of ζ implies that the constant steady state a_0 is real-valued and $A = a_0^2$ satisfies

$$f = (1 + \sigma r \tau A^2 + rA)\sqrt{A}.$$

Thus, $(\sqrt{A}, r\tau A^2) \in \mathbb{R} \times \mathbb{R}$ is a real-valued steady state of (2). Second, by slightly adjusting the forcing f , we may assume that $\sqrt{A/d} \in \mathbb{N}$. As a consequence, we obtain that $\Delta = 0$ in Theorem 1. These observations lead to the following corollary.

Corollary 1 *Let $d, \sigma, \tau > 0, \mu, v \in \mathbb{R}, r \in (0, 1/\sqrt{3})$. Assume that $(\sqrt{A}, r\tau A^2) \in \mathbb{R} \times \mathbb{R}$ is a real-valued steady-state of (3) with $f = (1 + \sigma r \tau A^2 + rA)\sqrt{A}$, $\zeta = A - \sigma\mu r\tau A^2$*

such that $\sqrt{A/d} \in \mathbb{N}$. Then the steady state $(\sqrt{A}, r\tau A^2) \in \mathbb{R} \times \mathbb{R}$ is spectrally unstable provided there exists $\epsilon > 0$ such that the following three conditions hold:

$$\sigma\tau < \frac{1}{(1+\epsilon)4r} \left(\sqrt{1+r^2} - 2r \right)^2 \quad (13)$$

and

$$A \in (\tilde{\xi}_1(\epsilon), \tilde{\xi}_2(\epsilon)) \quad (14)$$

where $0 < \tilde{\xi}_1(\epsilon) < \tilde{\xi}_2(\epsilon)$ are the positive roots of the polynomial

$$\tilde{q}(\xi) := -1 - \epsilon + (\sqrt{1+r^2} - 2r)\xi - \sigma r \tau \xi^2,$$

and

$$\left(\epsilon + \frac{|\omega_1| + |\omega_4|}{\epsilon} \right)^2 < \left(-1 + (\sqrt{1+r^2} - 2r)A - \sigma r \tau A^2 + \frac{1}{\tau} \right)^2 + \frac{v^2 A}{d} \quad (15)$$

where

$$\omega_1 := \frac{2\sigma r A^2}{(1+r^2)} \left((r - \mu)\sqrt{1+r^2} - (1+r^2) \right),$$

$$\omega_4 := \frac{2\sigma r A^2}{(1+r^2)} \left((\mu - r)\sqrt{1+r^2} - (1+r^2) \right).$$

Moreover the instability is found for modes with wave number $k^* = \sqrt{A/d}$.

2.2 Numerical illustration

Here we present numerical computations of the instability region as established in Corollary 1. Motivated by [24] we fix the values of the physical quantities as $d = 0.025, \sigma = 0.5, \mu = 1, v = 190$. The parameter $\epsilon > 0$ is a free parameter (in principle). However, small values of ϵ typically lead to larger regions where instability is guaranteed. Numerical experiments showed that our choice of $\epsilon = 0.05$ led to good results (see discussion below).

The numerical algorithm is as follows. For a given $0 < r < 1/\sqrt{3}$ and $0 < \tau$ we check the condition (13). If it is satisfied, we compute the smallest number $A \in (\tilde{\xi}_1(\epsilon), \tilde{\xi}_2(\epsilon))$ such that $\sqrt{A/d} \in \mathbb{N}$ and set $f := (1 + \sigma r \tau A^2 + rA)\sqrt{A}$ $\zeta := A - \sigma \mu r \tau A^2$. Then $(\sqrt{A}, r\tau A^2) \in \mathbb{R} \times \mathbb{R}$ is a constant steady-state. If the remaining conditions (13), (15) of Corollary 1 are met, we indicate this by a colored dot in the $r - \sigma\tau$ plane¹, where the color encodes the value of the forcing f^2 . Note that our choice of A yields the minimum value of f such that all conditions of Corollary 1

¹ We scale the y-axis by σ to improve readability of the plots.

are satisfied, and we therefore refer to it as the threshold power, denoted by f_{thres} . The result is depicted in the left panel of Fig. 1.

Corollary 1 provides only a sufficient condition for instability so that the threshold power f may be overestimated while the instability region may be underestimated. We therefore wanted to see how well Corollary 1 predicts the full instability region. To illustrate this we computed the eigenvalues of L_{2,k^*} (see the proof of Theorem 1) for k^* as Corollary 1 and where the forcing is treated as a free parameter (which in turn determines a_0 and ζ). The minimal necessary forcing values which leads to an eigenvalue with positive real parts is called f_{num} . The result is shown in the right panel of the Figure 1. The difference $f_{\text{thres}}^2 - f_{\text{num}}^2 \geq 0$ for each tuple $(r, \sigma\tau)$ of the instability region is shown in the bottom panel of Figure 1. Our conclusions are the following:

- (i) the shape of the instability region as predicted by the analytical results of Corollary 1 (left panel) is in very good agreement with the numerically computed instability region (right panel),
- (ii) both results are also in good agreement with [24],
- (iii) quantitatively, the values of f_{thres} and f_{num} agree well in large parts of the instability region but differ more significantly near its border (which is to be expected since there f_{num} and f_{thres} both tend to infinity).

Similarly, in Figure 2, computations are presented for $\mu = -1$ while leaving all other parameters unchanged.

3 Existence of non-homogeneous solutions

This section is devoted to the existence of non-constant 2π -periodic solutions of

$$\begin{aligned} -da'' + (\zeta - i - (i\sigma - \mu)n - (1 + ir)|a|^2)a + if &= 0, \\ vn' + \frac{n}{\tau} - r|a|^4 &= 0, \end{aligned} \tag{16}$$

which yield space-periodic and, in the case of the free carriers via $N(x, t) := n(x + vt)$ also time-periodic solutions of (3).

Remark 3 In (16) we write the coupling constant as $i\sigma - \mu$ instead of $\sigma(i - \mu)$ which is more suitable for our purposes. Clearly, both choices of couplings are equivalent provided $\sigma \neq 0$.

In the following, our considerations are divided into three parts. In the first part, we exploit continuation methods based on the Implicit Function Theorem to establish Theorem 3, which is our main result on the existence of non-constant solutions of (16). In the second part, we present numerical simulations of non-constant solutions illustrating the findings of Theorem 3. Both, the analytical and the numerical existence analysis require that a continuability condition is satisfied.

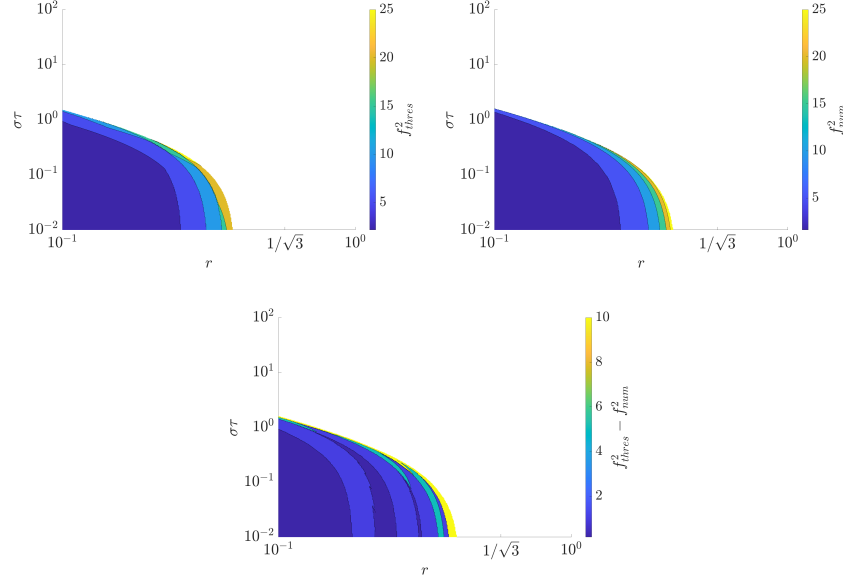


Fig. 1 Illustration of the instability region in the $r - \sigma\tau$ -plane with the threshold power encoded by the different colors. Parameters are set to $d = 0.025$, $\sigma = 0.5$, $\mu = 1$, $v = 190$, $\epsilon = 0.05$. The left panel shows the instability region predicted by Corollary 1. The right panel displays instability region obtained by numerical approximations of unstable eigenvalues of L_{2,k^*} . The bottom panel shows the difference between f_{thres} and f_{num} .

In the last part, we give a detailed discussion of this condition in the limit where damping, forcing, and the two-photon absorption are small.

3.1 Continuation analysis for non-homogeneous solutions

We continue to use the notation of Section 3, in particular \mathbb{T} is the one dimensional torus of length 2π . We consider all function spaces as vector spaces over the field \mathbb{R} and we use on $L^2(\mathbb{T})$ the scalar product $\langle f, g \rangle_{L^2} = \text{Re} \int_{\mathbb{T}} f \bar{g} dx$.

Since the equation for n is a linear first order inhomogeneous ODE with periodicity condition in x we can solve it by the Duhamel formula. More precisely, for fixed $a \in H^2(\mathbb{T})$ the solution of the ODE for n is given by

$$\mathcal{N}(a) = r \left(v \partial_x + \frac{1}{\tau} \right)^{-1} |a|^4.$$

The solution operator \mathcal{N} can be computed explicitly as a non-local integral operator, which is given by the following expression:

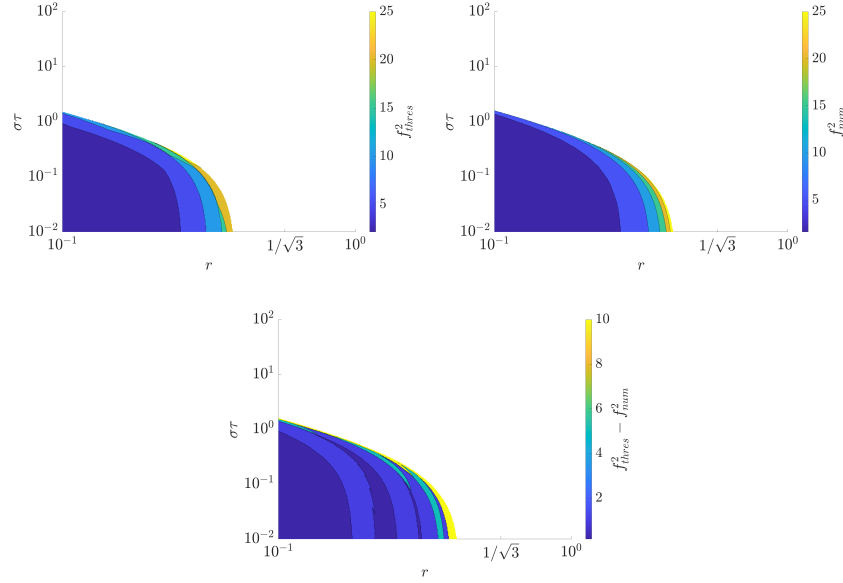


Fig. 2 This figure shows computations of the instability region as in Fig. 1 for the TPA parameter $\mu = -1$, while leaving all other parameters unchanged.

$$\mathcal{N} : \begin{cases} H^1(\mathbb{T}) \rightarrow H^2(\mathbb{T}), \\ \mathcal{N}(a)(x) := \frac{\tau}{v} \left(\frac{1}{e^{\frac{2\pi}{\tau v}} - 1} \int_0^{2\pi} e^{\frac{(y-x)}{\tau v}} |a(y)|^4 dy + \int_0^x e^{\frac{(y-x)}{\tau v}} |a(y)|^4 dy \right), \end{cases} \quad (17)$$

and allows us to write (16) in the compact form

$$-da'' + (\zeta - i - (i\sigma - \mu)\mathcal{N}(a) - (1 + ir)|a|^2)a + if = 0. \quad (18)$$

For $\sigma = \mu = 0$, (18) becomes

$$-da'' + (\zeta - i - (1 + ir)|a|^2)a + if = 0 \quad (19)$$

and the existence of non-constant periodic solutions of (19) is proven in [5] provided that the nonlinear damping parameter satisfies $0 \leq r \leq r_*$. The value of r_* is available explicitly and satisfies $r_* \in (0, 1/\sqrt{3})$ provided that $f^2 \geq 1$. We start with such a solution under the assumption of its non-degeneracy according to the following definition.

Definition 1 A non-constant solution $a_0 \in H^2(\mathbb{T})$ of (19) is called non-degenerate if the kernel of the linearized operator

$$\mathcal{L}_0\phi = -d\phi'' + (\zeta - i - 2(1 + ir)|a_0|^2)\phi - (1 + ir)a_0^2\bar{\phi}, \quad \phi \in H^2(\mathbb{T}) \quad (20)$$

satisfies $\text{Ker}(\mathcal{L}_0) = \text{Span}\{a'_0\}$.

Remark 4 Note that $\mathcal{L}_0 : H^2(\mathbb{T}) \rightarrow L^2(\mathbb{T})$ is a compact perturbation of the isomorphism $-d\partial_x^2 + \text{sign}(d) : H^2(\mathbb{T}) \rightarrow L^2(\mathbb{T})$ and hence an index-zero Fredholm operator. Notice also that $\text{Span}\{a'_0\}$ always belongs to the kernel of \mathcal{L}_0 due to translation invariance in x of (19). Non-degeneracy means that except for the obvious candidate a'_0 (and its real multiples) there is no other element in the kernel of \mathcal{L}_0 .

Our strategy is to show that non-constant, non-degenerate solutions of (19) as in Definition 1 can be continued into the regime of $(\sigma, \mu) \neq (0, 0)$ provided that a continuability condition is satisfied. Before we state our existence result, we note that the non-degeneracy assumption implies that the adjoint operator $\mathcal{L}_0^* : H^2(\mathbb{T}) \rightarrow L^2(\mathbb{T})$ also has a one-dimensional kernel and thus there exists $a_0^* \in H^2(\mathbb{T})$ such that $\text{Ker}(\mathcal{L}_0^*) = \text{Span}\{a_0^*\}$.

Theorem 3 *Let $d, \tau, v \neq 0$, $\zeta, f \in \mathbb{R}$, $r > 0$ be fixed and $a_0 \in H^2(\mathbb{T})$ be a non-degenerate solution of (19) as in Definition 1. Assume that*

$$\alpha := \int_0^{2\pi} \mathcal{N}(a_0)a_0\bar{a}_0^* dx \neq 0,$$

where \mathcal{N} is the integral operator defined in (17). Then the following is true:

- (i) *If $\text{Re } \alpha \neq 0$, then there exist $\sigma^* > 0$ and a continuously differentiable curve $(-\sigma^*, \sigma^*) \ni \sigma \mapsto (\mu(\sigma), a(\sigma)) \in \mathbb{R} \times H^2(\mathbb{T})$ such that $a(\sigma)$ is a non-trivial solution of (18) for the coupling parameters $\sigma, \mu(\sigma)$ and*

$$\mu(0) = 0, \quad \|a(\sigma) - a_0\|_{H^2} = O(|\sigma|) \quad \text{as } \sigma \rightarrow 0.$$

Moreover, $\mu'(0) = -\text{Im } \alpha / \text{Re } \alpha$.

- (ii) *If $\text{Im } \alpha \neq 0$, then there exist $\mu^* > 0$ and a continuously differentiable curve $(-\mu^*, \mu^*) \ni \mu \mapsto (\sigma(\mu), a(\mu)) \in \mathbb{R} \times H^2(\mathbb{T})$, such that $a(\mu)$ is a non-trivial solution of (18) for the coupling parameters $\sigma(\mu), \mu$ and*

$$\sigma(0) = 0, \quad \|a(\mu) - a_0\|_{H^2} = O(|\mu|) \quad \text{as } \mu \rightarrow 0.$$

Moreover, $\sigma'(0) = -\text{Re } \alpha / \text{Im } \alpha$.

Proof. We seek solutions of (18) of the form

$$a = a_0 + b, \quad \text{with } b \in H^2(\mathbb{T}) : b \perp_{L^2} a'_0.$$

After defining the space $X_0 := \text{Span}\{a'_0\}^{\perp_{L^2}} \cap H^2(\mathbb{T})$ this means that $b \in X_0$. Plugging the ansatz into (18) yields

$$\mathcal{F}(b, \sigma, \mu) := \mathcal{L}_0 b - (1 + ir)\mathcal{R}(b) - (i\sigma - \mu)\mathcal{N}(a_0 + b)(a_0 + b) = 0,$$

where \mathcal{L}_0 is the linearization about a_0 such that $\text{Ker}(\mathcal{L}_0) = \text{Span}\{a'_0\}$ by our non-degeneracy assumption and

$$\mathcal{R}(b) := \bar{a}_0 b^2 + 2a_0 |b|^2 + |b|^2 b.$$

Note that $\mathcal{F} \in C^1(X_0 \times \mathbb{R} \times \mathbb{R}, L^2(\mathbb{T}))$. Next, we use the Lyapunov-Schmidt reduction to find non-trivial solutions of the equation $\mathcal{F}(b, \sigma, \mu) = 0$. Let us define the orthogonal projections

$$P : L^2(\mathbb{T}) \rightarrow \text{Span}\{a_0^*\} \quad \text{and} \quad P^\perp := I - P : L^2(\mathbb{T}) \rightarrow \text{Span}\{a_0^*\}^\perp = \text{Ran}(\mathcal{L}_0).$$

Then, $\mathcal{F}(b, \sigma, \mu) = 0$ is equivalent to the system

$$P^\perp \mathcal{F}(b, \sigma, \mu) = 0, \tag{21}$$

$$P \mathcal{F}(b, \sigma, \mu) = 0, \tag{22}$$

which we solve subsequently. Consider the auxiliary function

$$\mathcal{G} : X_0 \times \mathbb{R} \times \mathbb{R} \rightarrow \text{Ran}(\mathcal{L}_0) = \text{Span}\{a_0^*\}^\perp, \quad \mathcal{G}(b, \sigma, \mu) := P^\perp \mathcal{F}(b, \sigma, \mu).$$

Then, \mathcal{G} is continuously differentiable, $\mathcal{G}(0, 0, 0) = 0$, and

$$\partial_b \mathcal{G}(0, 0, 0) = P^\perp \mathcal{L}_0 : X_0 \rightarrow \text{Span}\{a_0^*\}^\perp$$

is an isomorphism by construction. The Implicit Function Theorem yields that there exist open neighborhoods $U \subset X_0$ of 0, $V \subset \mathbb{R}^2$ of 0 and a continuous differentiable map $V \ni (\sigma, \mu) \rightarrow b(\sigma, \mu) \in U$ such that $b(0, 0) = 0$ and

$$\begin{aligned} (b, (\sigma, \mu)) \in U \times V \text{ solves } \mathcal{G}(b, \sigma, \mu) = 0 \\ \Leftrightarrow (\sigma, \mu) \in V, \quad (b, \sigma, \mu) = (b(\sigma, \mu), \sigma, \mu). \end{aligned}$$

This means that for $(\sigma, \mu) \in V$ the triple $(b(\sigma, \mu), \sigma, \mu)$ solves (21). We substitute the triple $b(\sigma, \mu), \sigma, \mu$ into the bifurcation equation (22) to find

$$P \mathcal{F}(b(\sigma, \mu), \sigma, \mu) = 0.$$

The equation is equivalent to the 2-dimensional problem $g(\sigma, \mu) = 0$ where

$$g(\sigma, \mu) := \langle (1 + i\sigma)\mathcal{R}(b(\sigma, \mu)) + (i\sigma - \mu)\mathcal{N}(a_0 + b(\sigma, \mu))(a_0 + b(\sigma, \mu)), a_0^* \rangle_{L^2}.$$

It is straight forward to check that $g(0, 0) = 0$ and

$$\nabla g(0, 0) = - \begin{bmatrix} \text{Im } \alpha \\ \text{Re } \alpha \end{bmatrix}.$$

Now, the assertions of Theorem 3 follow directly by another application of the Implicit Function Theorem to the problem $g(\sigma, \mu) = 0$ which finishes the proof. \square

3.2 Numerical illustration of the existence result

In the following, we describe an algorithm to numerically approximate the solution curve obtained in Theorem 3. Our method relies upon the continuation and bifurcation algorithm of the Matlab package `pde2path`, cf. [26]. We recall that the continuation procedure of Theorem 3 requires a non-trivial 2π -periodic starting solution a_0 of (19). Such solutions can be found numerically from bifurcations of the curve of constant solutions of (19) parameterized by ζ and we refer to [5] for a detailed numerical bifurcation analysis of (19).

For the first step of our algorithm, we fix the parameters d, ζ, f, r, τ, v and compute a non-trivial starting solution a_0 of (19). In the second step, we implement the orthogonality condition $\langle b, a'_0 \rangle_{L^2} = 0$ and perform a two parameter continuation in the parameters σ, μ , which yields a curve of solutions to (16). Projecting this curve onto the σ - μ -plane yields the result depicted in Fig. 3, where each point on this curve now corresponds to an approximation of a non-homogeneous solution of (16). The top and right inserts of the figure display profiles of the approximated solutions for $\sigma\mu \neq 0$, and the bottom insert corresponds to the solution a_0, n_0 at the bifurcation point. Note that the free carrier densities n can be computed by applying a discretized version of the solution operator (17) to the functions a . In this example the solution curve only exists if $\sigma\mu \leq 0$. The questions whether non-constant solutions also exist if $\sigma\mu > 0$ remains open, even after performing numerous simulations for different configurations of parameters and starting points a_0 .

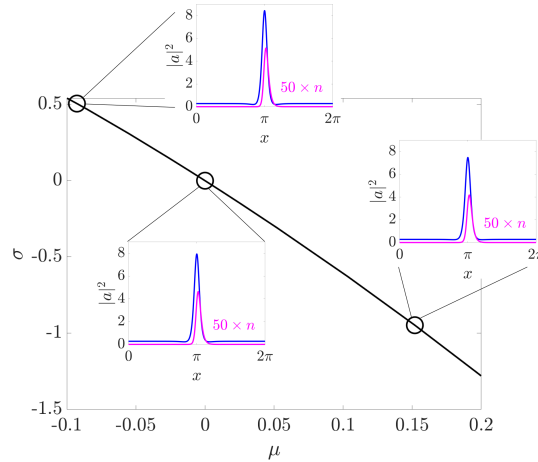


Fig. 3 Bifurcation diagram with inserts of solution profiles of (a, n) . Parameters: $d = 0.1, \zeta = 3.9, f = 2, r = 0.02, \tau = 0.1, v = 1$.

3.3 Continuability condition in the limit of small damping and forcing

The continuability condition $\alpha \neq 0$ of Theorem 3 becomes more explicit in the limit of small damping and forcing and small two-photon absorption. This means that instead of (16) we consider now

$$\begin{aligned} -da'' + (\zeta - i\epsilon - (i\sigma - \mu)n - (1 + i\epsilon r)|a|^2)a + i\epsilon f &= 0, \\ vn' + \frac{n}{\tau} - \epsilon r|a|^4 &= 0, \end{aligned} \quad (23)$$

with $|\epsilon| \ll 1$. By resolving the second equation in (25) we obtain the compact form

$$-da'' + (\zeta - i\epsilon - (i\sigma - \mu)\mathcal{N}_\epsilon(a) - (1 + i\epsilon r)|a|^2)a + i\epsilon f = 0 \quad (24)$$

where we have set $\mathcal{N}_\epsilon = \epsilon\mathcal{N}$ while we have kept Definition 17 for \mathcal{N} . Let $a_0 \in H^2(\mathbb{T})$ be a non-degenerate solution of

$$-da'' + (\zeta - i\epsilon - (1 + i\epsilon r)|a|^2)a + i\epsilon f = 0, \quad |\epsilon| \ll 1. \quad (25)$$

Using regular perturbation theory, we expand a_0 in powers of ϵ :

$$a_0 = a_{00} + \epsilon a_{01} + \mathcal{O}(\epsilon^2), \quad (26)$$

where a_{00} is a solution of the nonlinear Schrödinger equation

$$-da'' + \zeta a - |a|^2 a = 0$$

and a_{01} is found from the linear inhomogeneous equation

$$-da_{01}'' + \zeta a_{01} - 2|a_{00}|^2 a_{01} - a_{00}^2 \bar{a}_{01} = i(1 + r|a_{00}|^2)a_{00} - if.$$

In particular, (26) yields an expansion of a_0^* of the form

$$a_0^* = a_{00}' + \mathcal{O}(|\epsilon|)$$

allowing us to obtain an expansion of α in ϵ :

$$\begin{aligned} \alpha &= \int_0^{2\pi} \mathcal{N}_\epsilon(a_0) a_0 \bar{a}_0^* dx \\ &= \int_0^{2\pi} \epsilon \mathcal{N}(a_{00}) a_{00} \bar{a}_{00}' dx + \mathcal{O}(\epsilon^2) \\ &= -\frac{1}{2} \int_0^{2\pi} \epsilon \partial_x \mathcal{N}(a_{00}) |a_{00}|^2 dx + \mathcal{O}(\epsilon^2) \\ &= \frac{1}{2} \left(\frac{1}{\tau v} \int_0^{2\pi} \epsilon \mathcal{N}(a_{00}) |a_{00}|^2 dx - \frac{\epsilon r}{v} \|a_{00}\|_{L^6}^6 \right) + \mathcal{O}(\epsilon^2). \end{aligned}$$

A sufficient condition for $\alpha \neq 0$ is that

$$\begin{aligned} & \frac{1}{e^{\frac{2\pi}{\tau v}} - 1} \int_0^{2\pi} \int_0^{2\pi} e^{\frac{(y-x)}{\tau v}} |a_{00}(y)|^4 dy |a_{00}(x)|^2 dx \\ & + \frac{1}{\tau v} \int_0^{2\pi} \int_0^x e^{\frac{(y-x)}{\tau v}} |a_{00}(y)|^4 dy |a_{00}(x)|^2 dx \neq \|a_{00}\|_{L^6}^6, \end{aligned}$$

provided that $\epsilon \neq 0$ is sufficiently small. Since the function $\phi : (0, \infty) \rightarrow \mathbb{R}$ defined by

$$\begin{aligned} \phi(\xi) := & \frac{\xi}{e^{2\pi\xi} - 1} \int_0^{2\pi} \int_0^{2\pi} e^{(y-x)\xi} |a_{00}(y)|^4 dy |a_{00}(x)|^2 dx \\ & + \xi \int_0^{2\pi} \int_0^x e^{(y-x)\xi} |a_{00}(y)|^4 dy |a_{00}(x)|^2 dx \end{aligned}$$

is in general not constant, $\alpha \neq 0$ can be achieved for suitable choices of the parameters τ, v .

In the limit $\tau v \rightarrow +\infty$ we find that $\alpha \neq 0$ further simplifies to

$$\|a_{00}\|_{L^4}^4 \|a_{00}\|_{L^2}^2 \neq 2\pi \|a_{00}\|_{L^6}^6. \quad (27)$$

This condition can be checked numerically or even analytically, e.g. for those solutions of NLS which are available in an explicit form. To illustrate usability, we present an example where we numerically verify (27) for the cnoidal wave solutions of NLS. Let us define

$$\phi(x, k) = \sqrt{2}k \frac{2K(k)}{\pi} \operatorname{cn} \left(\frac{2K(k)}{\pi} x, k \right),$$

where $\operatorname{cn}(\cdot, k)$ is the Jacobi elliptic function, $K(k)$ is the complete elliptic integral of the first kind, and $k \in (0, 1)$ is the elliptic modulus. We refer to [9] for precise definitions. Then, $\phi(\cdot, k)$ is a 2π -periodic solution of

$$-a'' + \zeta(k)a - a^3 = 0, \quad \text{where} \quad \zeta(k) = \frac{4K^2(k)(2k^2 - 1)}{\pi^2}.$$

Numerical simulations in Fig. 4 show that (27) is satisfied at least for all values of $\zeta \in [0, 2]$ and thus solutions a_0 of (25) close to the cnoidal waves can be continued to solutions of (23).

4 Conclusion

To summarize, we have studied dynamical and stationary aspects of the Lugiato-Lefever equation with two-photon absorption and free carriers. First, we obtained a

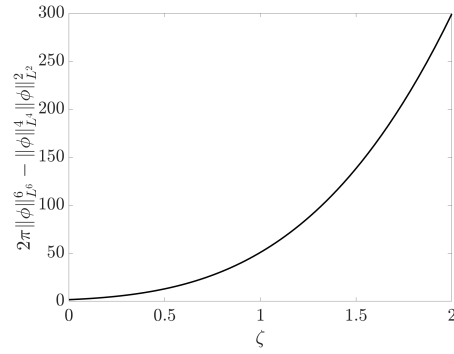


Fig. 4 Continuability condition (27) for cnoidal waves as a function of $\zeta = \zeta(k)$.

rigorous analytical result for modulation instability of constant steady states which is illustrated by numerical simulation of the instability region. Second, we gave an existence result for non-constant solutions in the range of small free-carrier parameters σ and μ . The results was illustrated by numerical simulations and continuability condition was verified in the small forcing, small damping, and small TPA limit. The following questions remain open:

- (i) Does modulation instability lead to the existence of stationary solutions? This is particularly interesting in the case $\mu\sigma > 0$ for which numerical results are not (yet) available. Note that the sign of $\mu\sigma$ is not determined by Theorem 3.
- (ii) What are the stability properties of the solutions obtained in Theorem 3?

Acknowledgements Funded by the Deutsche Forschungsgemeinschaft (DFG, German Research Foundation) – Project-ID 258734477 – SFB 1173.

References

1. Chembo, Y.K., Yu, N.: Modal expansion approach to optical-frequency-comb generation with monolithic whispering-gallery-mode resonators. *Physical Review A*, 82:033801, 2010.
2. Chembo, Y.K., Menyuk, C.R.: Spatiotemporal Lugiato-Lefever formalism for Kerr-comb generation in whispering-gallery-mode resonators. *Phys. Rev. A*, 87:053852 (2013).
3. Delcey, L., Haragus, M.: Periodic waves of the Lugiato-Lefever equation at the onset of Turing instability. *Philos. Trans. Roy. Soc. A*, 376(2117):20170188, 21 (2018).
4. Diddams, S.A., Udem, Th., Bergquist, J.C., Curtis, E.A., Drullinger, R.E., Hollberg, L., Itano, W.M., Lee, W.D., Oates, C.W., Vogel, K.R., Wineland, D.J., Reichert, J., Holzwarth, R.: An Optical Clock Based on a Single Trapped 199 Hg+ Ion. *Science (New York, N.Y.)*, 24(13):881–883 (1999).
5. Gärtner, J., Mandel, R., Reichel, W.: The Lugiato-Lefever Equation with Nonlinear Damping Caused by Two Photon Absorption. *J Dyn Diff Equat* 34, 2201–2227 (2022). <https://doi.org/10.1007/s10884-021-09943-x>
6. Geršchgorin, S.: Über die Abgrenzung der Eigenwerte einer Matrix, *Bulletin de l'Académie des Sciences de l'URSS. Classe des sciences mathématiques et na*, 1931, no. 6, 749–754
7. Godey, C.: A bifurcation analysis for the Lugiato-Lefever equation. *The European Physical Journal D*, 71(5), 131 (2017).
8. Godey, C., Balakireva, I.V., Coillet, A., Chembo, Y.K.: Stability analysis of the spatiotemporal Lugiato-Lefever model for Kerr optical frequency combs in the anomalous and normal dispersion regimes. *Phys. Rev. A*, 89:063814 (2014).
9. Gradshteyn, I. S., Ryzhik, I. M.: Table of integrals, series, and products, Translated from the Russian. Translation edited and with a preface by Daniel Zwillinger and Victor Moll. Eighth edition. Elsevier/Academic Press, Amsterdam, 2015. xlv+1133 pp. ISBN:978-0-12-384933-5
10. Hansson, T., Modotto, D., Wabnitz, S.: Dynamics of the modulational instability in microresonator frequency combs. *Phys. Rev. A*, 88:023819 (2013).
11. Hansson, T., Wabnitz, S.: Dynamics of microresonator frequency comb generation: Models and stability. *Nanophotonics*, 25(2), 231–243 (2016).
12. M. Haragus, M. A. Johnson, W. R. Perkins, and B. de Rijk: Nonlinear modulational dynamics of spectrally stable Lugiato-Lefever periodic waves. *Ann. Inst. H. Poincaré C Anal. Non Linéaire*, 40 (2023), pp. 769–802.
13. Herr, T., Hartinger, K., Riemensberger, J. Wang, C.Y., Gavartin, E., Holzwarth, R., Gorodetsky, M.L., Kippenberg, T.J.: Universal formation dynamics and noise of Kerr-frequency combs in microresonators. *Nature Photonics*, 6, 480–487 (2012).
14. Lau, R.K.W., Lamont, M.R.E., Okawachi, Y., Gaeta, A.L.: Effects of multiphoton absorption on parametric comb generation in silicon microresonators. *Opt. Lett.*, 40(12), 2778–2781 (2015).
15. Mandel, R., Reichel, W.: A priori bounds and global bifurcation results for frequency combs modeled by the Lugiato-Lefever equation. *SIAM J. Appl. Math.*, 77(1), 315–345 (2017).
16. Marin-Palomo, P., Kemal, J.N., Karpov, M., Kordts, A., Pfeifle, J., Pfeiffer, M.H.P., Trocha, P., Wolf, S., Brasch, V., Anderson, M.H., Rosenberger, R., Vijayan, K., Freude, W., Kippenberg, T.J., Koos, C.: Microresonator-based solitons for massively parallel coherent optical communications. *Nature*, 546(7657), 274–279 (2017).
17. T. Miyaji, I. Ohnishi, and Y. Tsutsumi: Bifurcation analysis to the Lugiato-Lefever equation in one space dimension. *Phys. D*, 239 (2010), pp. 2066–2083.
18. Parra-Rivas, P., Gomila, D., Gelens, L., Knobloch, E.: Bifurcation structure of localized states in the Lugiato-Lefever equation with anomalous dispersion. *Phys. Rev. E*, 97(4):042204, 20 (2018).
19. Parra-Rivas, P., Gomila, D., Matias, M.A., Coen, S., Gelens, L.: Dynamics of localized and patterned structures in the Lugiato-Lefever equation determine the stability and shape of optical frequency combs. *Phys. Rev. A*, 89:043813 (2014).
20. Parra-Rivas, P., Knobloch, E., Gomila, D., Gelens, L.: Dark solitons in the Lugiato-Lefever equation with normal dispersion. *Phys. Rev. A*, 93(6), 1–17 (2016).

21. Stanislavova, M., Stefanov, A.G.: Asymptotic stability for spectrally stable Lugiato-Lefever solitons in periodic waveguides. *J. Math. Phys.*, 59(10):101502, 12 (2018).
22. Suh, M.G., Vahala, K.: Soliton Microcomb Range Measurement. *Science*, 887, 884–887 (2017).
23. Trocha, P., Karpov, M., Ganin, D., Pfeiffer, M.H.P., Kordts, A., Wolf, S., Krockenberger, J., Marin-Palomo, P., Weimann, C., Randel, S., Freude, W., Kippenberg, T.J., Koos, C.: Ultrafast optical ranging using microresonator soliton frequency combs. *Science*, 359(6378), 887–891 (2018).
24. Trocha, P., Gärtner, J., Marin-Palomo, P., Freude, W., Reichel, W., Koos, C.: Analysis of Kerr comb generation in silicon microresonators under the influence of two-photon absorption and fast free-carrier dynamics. *Phys. Rev. A* 103, 063515 (2021).
25. Udem, Th., R. Holzwarth, R., Hänsch, T.W.: Optical frequency metrology. *Nature*, 416(6877), 233–237 (2002).
26. Uecker, H., Wetzel, D., Rademacher, J.: Pde2path - A Matlab Package for Continuation and Bifurcation in 2D Elliptic Systems. *Numerical Mathematics: Theory, Methods and Applications*, 7(1), 58–106 (2014). doi:10.1017/S1004897900000295